Contrib Mineral Petrol (2007) 153:719–731
DOI 10.1007/s00410-006-0172-6

ORIGINAL PAPER

A complex magmatic system beneath the Devès volcanic field, Massif Central, France: evidence from clinopyroxene megacrysts

A. B. Woodland · P. J. Jugo

Received: 18 August 2006 / Accepted: 4 December 2006 / Published online: 23 January 2007

Abstract Clinopyroxene megacrysts and mineral aggregates with clinopyroxene occur in the volcanic deposits at Mont Briançon and Marais de Limagne, which are located in the northern part of the Devès volcanic field (Massif Central, France). The clinopyroxenes can be subdivided into five groups based upon their major and trace element chemistry. Types 1a, 1b and 1c have mg# ~0.80 and are relatively Al-rich and low in Na and Fe^{3+}. Subdivision into three groups is based on differing trace element signatures. Type 2 clinopyroxenes have mg# = 0.63–0.65 and higher Na and Fe^{3+} ($Fe^{3+}/\Sigma Fe > 0.4$) contents and may contain apatite inclusions. A type 3 megacryst is Fe-rich (mg# = ~0.52) and has the highest Na and Fe^{3+} contents, as well as containing titanite and apatite inclusions. High Fe^{3+} contents in all clinopyroxenes investigated emphasises the need to consider Fe^{3+}/Fe^{2+} when assessing the petrologic origin of such megacrysts. The large range in mg# means that the clinopyroxenes could not all have crystallised from the same melt; in fact comparison with the basanitic host lavas from the two localities reveal that nearly all of the megacrysts are xenocrystic in the strict sense. The clinopyroxenes are mostly genetically related, having crystallised from related melts within the magmatic system that had undergone various degrees of differentiation. Similarities in clinopyroxene chemistry indicate that both volcanic centres are linked to the same magmatic system at depth. Assessing the depth of crystallisation reveals that types 1a and 1b formed in the lithospheric mantle, near the asthenosphere–lithosphere boundary, whereas types 1c, 2 and 3 formed in crustal magma chambers or conduits. Eruption was induced by a pulse of Mg-rich magma from the asthenosphere that entered the existing magmatic system, entraining clinopyroxene as megacrysts at several stages of ascent, before erupting at the surface. The style of eruption at Mont Briançon (cinder cone) and Marais de Limagne (maar) is different and most likely reflects local differences in near-surface hydrology. The essentially identical variety in megacrysts at the two localities suggests that eruption must have been nearly contemporaneous.

Keywords Volcanism · Megacryst · Clinopyroxene · Massif Central · Trace elements · Geochemistry · Ferric iron

Communicated by J. Hoefs.

Electronic supplementary material The online version of this article (doi:10.1007/s00410-006-0172-6) contains supplementary material, which is available to authorized users.

A. B. Woodland (✉) · P. J. Jugo
Institut für Geowissenschaften, Universität Frankfurt,
Senckenberganlage 30, 60054 Frankfurt, Germany
e-mail: woodland@em.uni-frankfurt.de

P. J. Jugo
Department of Earth Sciences, Laurentian University,
935 Ramsey Lake Rd., P3E 2C6 Sudbury, ON, Canada

Introduction

Megacrysts of clinopyroxene, amphibole and occasionally phlogopite, apatite, feldspar and zircon are a common occurrence in alkaline basaltic lavas, where they may be accompanied by peridotite and pyroxenite xenoliths (e.g., Best 1970; Binns et al. 1970; Irving 1974; Wilkinson 1975; Gutmann 1977; Wass 1979;

Irving and Frey 1984; Liotard et al. 1983, 1988; Shaw and Eyzaguirre 2000; Akinin et al. 2005). The megacrysts can have a variety of origins. Megacrysts may be unrelated to the current volcanic system, having been entrained in the magma as xenocrysts or even originally as a xenolith that became disaggregated during transport (e.g., Schulze 1987). An exotic origin can generally be discerned geochemically or by comparison with experimentally determined phase relations. In some cases, the phases are in chemical equilibrium with the host lava so that they are essentially phenocrysts and their composition(s) provide a glimpse of magma chamber conditions prior to eruption (e.g., Liotard et al. 1988). In many other cases, megacrysts are interpreted to have crystallised at high pressures from magmas petrogenetically related to the host lavas (e.g., Irving and Frey 1984; Shaw and Eyzaguirre 2000). This interpretation is supported by the observation of mafic veins containing clinopyroxene, amphibole, and/or phlogopite of similar composition occurring in some mantle xenoliths, as well as in some orogenic lherzolite massifs (e.g., Wilshire et al. 1980; Bodinier et al. 1987; Witt-Eickschen et al. 1993; Woodland et al. 1996; Shaw and Eyzaguirre 2000). Having crystallised at depth over a variety of pressure and temperature conditions, these megacrysts can give us insights into the chemical evolution of the magmatic system and potentially provide us with important information about the ''plumbing'' and melt migration beneath a volcanic centre, even from mantle depths.

Alkali basaltic volcanism is widespread in the Massif Central, occurring as numerous small centres clustered into several fields (Brousse and Lefevre 1990). Along with peridotite and pyroxenite xenoliths, clinopyroxene and amphibole megacrysts are known to occur at a number of localities (Biovin 1982; Liotard et al. 1983, 1988). Liotard et al. (1988) investigated regional variations in lava and clinopyroxene chemistry rather than focussing on any particular locality in detail. As such, their work forms a useful starting point for this work. Two types of clinopyroxene megacrysts and phenocrysts were identified by Liotard et al. (1988): (1) aegerine-rich clinopyroxenes enriched in REE, which are considered to have crystallised at high pressures from differentiated lavas, and (2) aegerine-poor augites relatively low in REE and apparently in equilibrium with their host lavas. However, their assessment of ferric iron contents was based only on measurements made by atomic absorption spectrometry and the assumption of stoichiometry, an approach known to be subject to significant uncertainty (e.g., Canil and O'Neill 1996).

We have undertaken a detailed study of a suite of clinopyroxene (cpx) megacrysts and clinopyroxene aggregates from two well-known localities on the Devès plateau, Mont Briançon and Marais de Limagne. Our goal was to determine the origin of these clinopyroxenes and, if possible, to use them as a probe of the magmatic system at depth. A question we sought to address was whether or not there is a linkage between the two localities at depth. The suite of samples reveals a complex history of differentiation at various depths in the crust and mantle and provides evidence for the likely cause of the eruptions.

Geological background

The French Massif Central is a classic example of continental intraplate alkaline magmatism and is spatially related to the West-European Rift-System. Tertiary to recent volcanism has occurred in three phases (e.g., Wilson and Downes 1991; Michon and Merle 2001): (1) scattered volcanism in the northern part of the Massif Central between 65 and 38 Ma, (2) magmatism related to rifting and the formation of the Limagne graben, again restricted to the northern portion of the Massif Central (38–15 Ma), and (3) a major magmatic event from early Miocene to recent times that began in the south and spread to the north. Two peaks in activity occurred during this last phase (e.g., Brousse and Lefevre 1990; Wilson and Downes 1991; Michon and Merle 2001). The earliest produced the Cantal, Aubrac, Velay, and Coirons volcanic fields between ~10 and 5 Ma (Fig. 1). The second peak occurred in both the south and north of the Massif Central and formed the Devès and Mont Dore volcanic fields from 3.5–0.5 Ma. Other older volcanic fields were also locally active during this time. The most recent eruptions in the Massif Central are those in the Chaîne des Puys, the Cézallier and Bas-Vivrais (Brousse and Lefevre 1990; Goer et al. 1991). Uplift and rifting appears to be related to a mantle plume located at depth (e.g., Granet et al. 1995; Sobolev et al. 1996), which is also responsible for the alkaline volcanism in the region. An alternative hypothesis invokes thermal erosion of the lithosphere that was caused by asthenospheric flow, which was induced by the formation of the adjacent deep Alpine lithospheric root (Merle and Michon 2001).

Mont Briançon and Marais de Limagne are situated in the northern part of the Devès volcanic field, west of Le Puy en Velay. Lying between the Loire and Allier rivers, the plateau of the Devès covers an area of ca. 900 km^2 (60 × 15 km) and is elongated in a NW–SE direction, reflecting a structural control

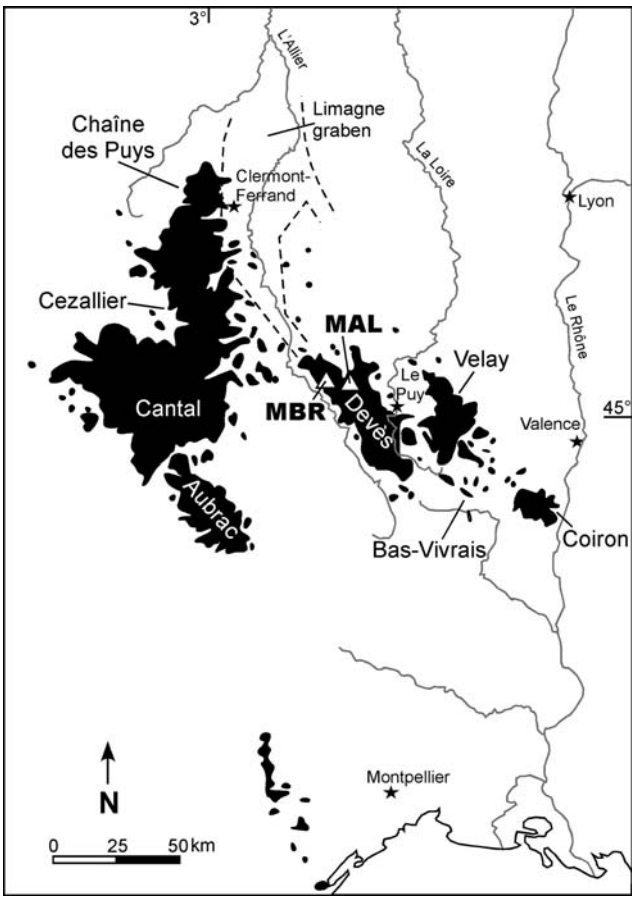

Fig. 1 Map showing the distribution of Tertiary to Holocene age volcanic fields of the Massif Central along with the location of Mont Briançon and Marais de Limagne in the Devès. Map modified after Debaisieux (1999)

through the southeastern extension of the Limagne graben (Fig. 1). The field comprises nearly 200 volcanic centres and is dominated by fissure eruptions that produced a ca. 20 km long ridge of nearly overlapping edifices, including Mont Devès. While Marais de Limagne lies at the northern end of this trend, Mont Briançon is displaced 3–4 km to the west. The volcanism is of Plio-Pleistocene age (Brousse and Lefevre 1990), with Mont Briançon reported to have an age of 1.6 ± 1 Ma (Lorand et al. 2003). The two localities are ~8 km from each other (Fig. 1). The lavas at both localities are nepheline-normative basanites containing 5–6 wt% $Na_2O + K_2O$ (Liotard et al. 1988). However, the style of volcanism is markedly different at the two localities. Mont Briançon is a cinder cone, made of massive vesicular scoria. Marais de Limagne is a maar, with lapilli tuffs deposited on the flanks. The maar formed in between two pre-existing cinder cones (Peterlongo and Goer de Herve 1978).

The samples

A total of 16 samples were studied, 10 from Mount Briançon (MBR) and 6 from Marais de Limagne (MAL). Most of the clinopyroxene megacrysts are dark glassy crystal fragments ranging from 8 to 15 mm in size (e.g., Fig. 2a). Some megacrysts are lozenge-shaped, exhibiting resorbed surfaces (Fig. 2b), while others are more angular in shape. Several other samples, MBR-2, MBR-3 and MBR-9 are vuggy, indicating reaction and melting enroute to the surface (Fig. 2c). Samples MBR-1, MBR-4 and MBR-5 contain euhedral apatite inclusions (Fig. 2a). MBR-4 also contains titanite inclusions. Sulphide blebs and rods occur in three samples (MAL-2, MAL-4, MAL-5, Fig. 2d). The sulphides are systematically distributed in domains within the megacryst, exhibiting a texture similar to that described by Peterson and Francis (1977) and Dromgroole and Pasteris (1987). Peterson and Francis (1977) interpreted this texture has been as having developed by droplets of immiscible sulphide liquids adhering to the surfaces of rapidly growing clinopyroxene crystals.

In addition to the megacryst fragments, two crystal aggregates were investigated. One sample from Mount Briançon (MBR-8) is an aggregate of coarse cpx (~800 μm) and olivine and one sample from Marais de Limagne is a fine aggregate of cpx and brown amphibole (MAL-3).

Analytical methods

Major element compositions of the megacrysts were determined using a JEOL JXA-8900RL electron microprobe operating at 15 kV accelerating voltage and a 20 nA beam current. A mix of natural and synthetic standards that yield reliable results for clinopyroxene and amphibole were employed. The analyses were all performed in wavelength-dispersive mode and a ZAF matrix correction was applied to the raw data collected. Mineral compositions are presented in Table 1.

Ferric iron contents were determined on optically clean handpicked separates by ^{57}Fe Mössbauer spectroscopy. Sufficient material was finely ground to prepare an absorber with a thickness of ~5 mg Fe/cm^2. For sample MBR-9 the amount of clean clinopyroxene obtained was too small to permit a ferric iron determination. The samples were mounted in a hole drilled in a Pb disc. A small amount of sugar was added to yield enough material to uniformly cover the sample holder and yet retain the desired thickness. A Ta-foil with a hole of appropriate diameter was used ensure

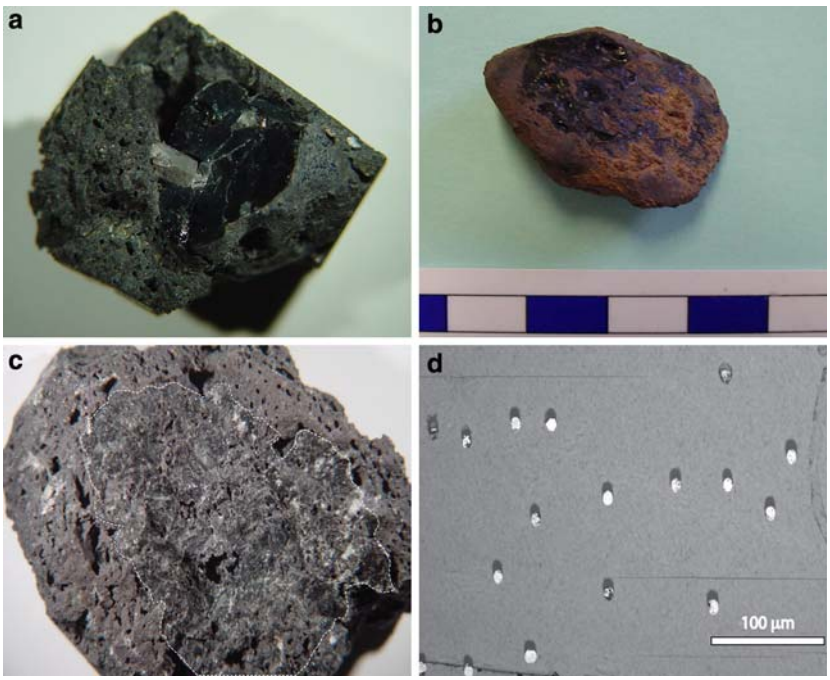

Fig. 2 Examples of the clinopyroxene megacrysts studied. **a** Sample MBR-1 is a fragment with some rounded margins and containing apatite inclusions. Long dimension is 8 mm, **b** sample MAL-1 exhibits a rounded, resorbed surface. Tick marks on the scale are in cm. **c** Sample MBR-2 is a clinopyroxene with a vuggy texture and irregular surface, highlighted with a *dashed line*. Long dimension of the clinopyroxene is 22.5 mm. **d** Reflected-light micrograph of sulphide inclusions in megacryst sample MAL-2. Note the *rod-shaped* form

Table 1 Major element compositions of clinopyroxene, olivine and amphibole

Mineral/ type	MBR-1 type2	MBR-2 type1c	MBR-3 type1c	MBR-3 olivine	MBR-4 type3	MBR-5 type2	MBR-6 type2	MBR-8 type1a	MBR-9 type1a	MBR-10 type1b	MBR-11 type2
CaO	20.38	21.38	21.32	0.11	20.09	20.49	20.46	20.05	21.42	18.63	20.35
TiO_2	1.55	1.06	1.20	0.03	2.09	1.56	1.97	1.38	1.42	1.62	1.56
Cr_2O_3	ND	0.10	0.13	ND	ND	ND	ND	0.18	0.27	0.03	ND
MnO	0.27	0.14	0.15	0.21	0.41	0.26	0.22	0.11	0.14	0.13	0.25
FeO	10.52	6.26	6.26	16.84	12.96	10.48	10.42	5.80	5.37	6.92	10.62
NiO	ND	ND	ND	0.13	ND	ND	ND	0.02	0.04	ND	ND
Na_2O	1.80	1.02	1.09	0.04	2.19	1.74	1.68	1.04	0.78	1.26	1.70
SiO_2	48.08	50.01	49.59	40.04	46.03	48.59	47.11	49.64	49.82	48.77	49.12
Al_2O_3	5.74	5.46	6.31	0.05	7.48	5.70	7.03	7.67	6.26	8.71	5.80
MgO	10.71	13.68	13.31	43.53	7.78	10.36	10.04	14.03	14.27	13.40	10.34
Total	99.05	99.12	99.37	100.98	99.04	99.18	98.93	99.92	99.79	99.48	99.74
$Fe^{3+}/\Sigma Fe$[a]	0.421	0.271	0.291		0.419	0.439	0.433	0.296		0.318	0.392
mg#	0.64	0.80	0.79	0.82	0.52	0.64	0.63	0.81	0.83	0.78	0.63

	MAL-1 type 1a	MAL-2 type 1b	MAL-3 type 1c	MAL-3 amph	MAL-4 type 1b	MAL-5 type 1b	MAL-7 type 2
K_2O				1.45			
CaO	20.24	18.59	20.81	11.28	18.66	18.91	20.27
TiO_2	1.55	1.66	1.06	3.88	1.67	1.74	1.61
Cr_2O_3	0.02	ND	0.30	0.28	0.04	ND	ND
MnO	0.12	0.14	0.15	0.11	0.18	0.14	0.26
FeO	5.81	6.72	6.41	9.37	6.76	6.73	10.76
NiO	0.02	0.03	0.04	0.05	ND	ND	ND
Na_2O	1.08	1.29	1.12	2.61	1.35	1.23	1.87
SiO_2	48.47	47.93	49.92	41.14	47.83	47.54	48.10
Al_2O_3	8.76	9.14	5.84	13.28	8.97	9.27	6.23
MgO	13.65	13.27	13.21	13.67	13.14	13.30	9.93
Total	99.72	98.77	98.86	97.12	98.60	98.87	99.05
$Fe^{3+}/\Sigma Fe$	0.397	0.341	0.302	0.532	0.387	0.378	0.422
mg#	0.81	0.78	0.79	0.72	0.78	0.78	0.62

ND not detected, detection limits for Cr and Ni are 190 and 200 ppm, respectively

[a] From Mössbauer spectroscopy

that only gamma rays that had interacted with the sample reached the detector. Spectra were obtained at room temperature, in transmission mode on a constant acceleration Mössbauer spectrometer with a nominal 50 mCi ^{57}Co source in a 6 μm Rh matrix. The velocity scale was calibrated relative to 25-μm thick α-Fe foil at room temperature using the positions certified by NIST. Mirror image spectra were collected over 512 channels with a velocity range of ±5 mm/s. The spectra were fit with the NORMOS software package (distributed by Wissenschaftliche Elektronik GmbH, Germany).

Spectra from clinopyroxene were fit following the approach successfully applied by Woodland et al. (2006) for mantle clinopyroxenes, which is similar to the spectral model adopted by many others (e.g., Luth and Canil 1993; Canil and O'Neill 1996; McCammon et al. 1998; Sobolev et al. 1999). The spectra were fit with two quadrupole split doublets for Fe^{2+} and one doublet for Fe^{3+}, each with Lorentzian peak shapes and equal areas (Fig. 3). Peak widths were allowed to vary for the Fe^{2+} doublets, to help account for next nearest neighbour effects. As a result of the relatively high Fe^{3+} contents in the samples investigated here, uncertainties in $Fe^{3+}/\Sigma Fe$ are estimated to be ±0.010 in absolute terms and uncertainties in the hyperfine parameters are in the range of ±0.02 for both the Fe^{2+} and Fe^{3+} doublets. The spectrum of amphibole from sample MAL-3 was fit following the same procedure as for clinopyroxene.

Trace element concentrations were determined by LA-ICP-MS on either thick sections or on polished fragments mounted in epoxy. A New Wave UP-213 (wavelength = 213 nm) laser system combined with a ThermoFinnigan ELEMENT 2 ICP-MS at the Institut für Geowissenschaften in Frankfurt was used for the measurements. The samples were analysed using an 80 μm spot and 0.15 mJ energy at 10 Hz. The NIST SRM 612 standard glass was used for the external calibration of the 28 elements listed in eTable 2. The reference values were taken from Pearce et al. (1997). Calcium was used for internal standardisation. A gas blank was measured before every measurement. The raw data were exported from the ICP-MS and processed using Glitter 4.0 (Van Achterberg et al. 2001). Based upon values of the standard measured intermittently during data acquisition, analytical accuracy and precision is ~5% for most trace elements, except for Be and V, which have uncertainties of ~10%.

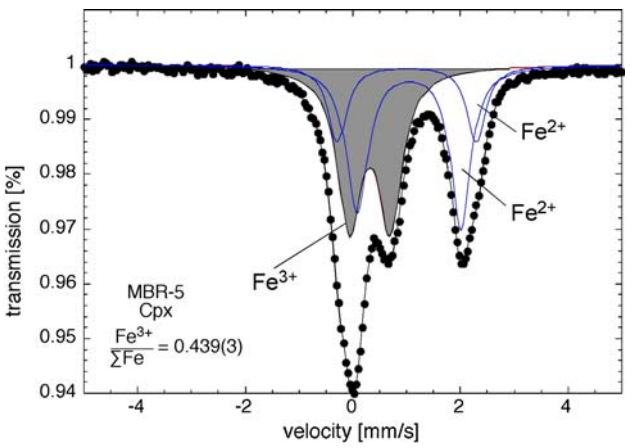

Fig. 3 Mössbauer spectrum of clinopyroxene megacryst MBR-5. The Fe^{3+} component of the spectrum is denoted in *grey*

Clinopyroxene composition

Major elements

As is commonly observed for megacrysts, the individual clinopyroxenes are compositionally homogeneous (Fig. 4). Chemical compositions are provided in Table 1a and b. All clinopyroxenes are Cr-poor (<0.3 wt% Cr_2O_3), with most having Cr-contents at or near the detection limit. Three broad populations can be discerned on the basis of mg# [molar Mg/(Mg + Fe_{total})] and differing major element compositions and are referred to here as type 1, 2 and 3 clinopyroxenes (see e.g., Fig. 5a). The most Mg-rich are the type 1 clinopyroxenes, having mg# ~0.80. They are relatively Al-rich and low in Na and Fe^{3+}. Measured $Fe^{3+}/\Sigma Fe$ are typically ~0.3, although several samples from Marias de Limagne are richer in Fe^{3+} (Table 1). In all cases, Na cations per formula unit (pfu) exceed Fe^{3+} contents (eTable 1), implying the presence of Na-bearing components in addition to an aegerine component (i.e., $NaAlSi_2O_6$). Type 1 clinopyroxenes dominate the sample set from Marais de LImagne, with three of these megacrysts containing blebs and rods of (Fe,Ni)S. Type 2 clinopyroxenes have mg# = 0.63–0.65 and higher Na and Fe^{3+} ($Fe^{3+}/\Sigma Fe > 0.4$) contents than the type 1 samples. Most of these samples are from Mont Briançon, although MAL-7, from MAL, also belongs to this group. Several megacrysts contain inclusions of euhedral apatite (MBR-1, MBR-5). One megacryst (MBR-4) has a mg# = ~0.52 and contains titanite as well as apatite inclusions. This clinopyroxene also has the highest Na and Fe^{3+} contents and has been designated as type 3. In contrast to the type 1 clinopyroxenes, types 2 and 3 have Fe^{3+} cations (pfu) in excess to that of Na (eTable 1). This implies that Na incorporation in these latter types was crystal chemically controlled by the presence of Fe^{3+} and that

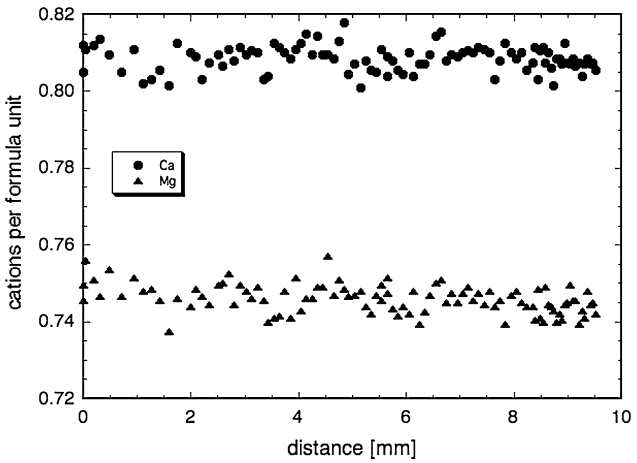

Fig. 4 Rim to rim compositional profiles of Mg and Ca across sample MAL-1 illustrating the degree of homogeneity in the megacrysts. This megacryst is nearly 1 cm in diameter

additional Fe^{3+} was balanced by other cation substitutions, such as [^{4}Al]. Chemical compositions are consistent with this assessment (eTable 1). In accord with previous studies (Canil and O'Neill 1996; Sobolev et al. 1999; Woodland et al. 2006), our data provide further evidence for the necessity to directly measure Fe^{3+} contents in clinopyroxene, rather than relying on structural formula calculations based upon microprobe data alone.

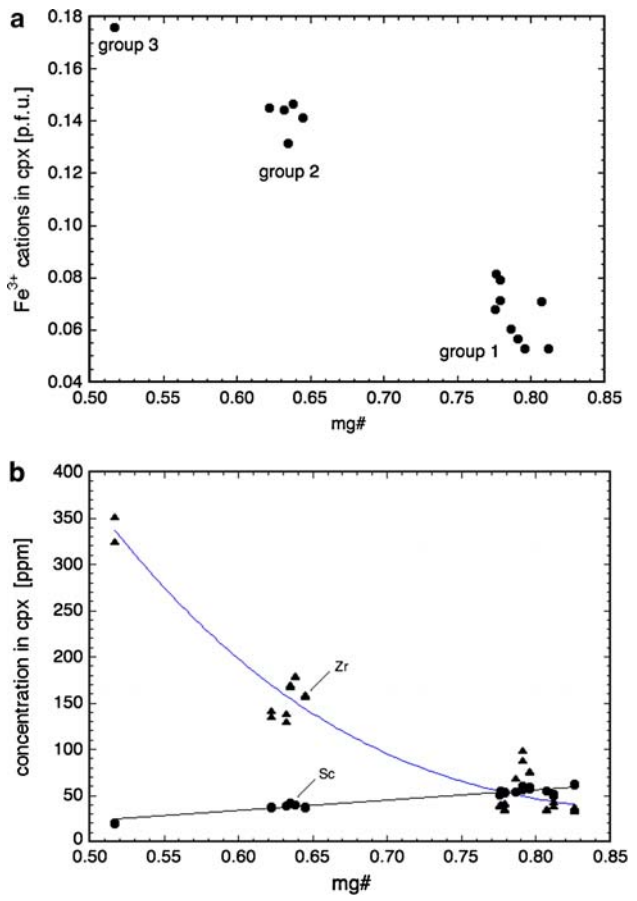

Fig. 5 Variation in **a** Fe^{3+} (in cations per formula unit), **b** Zr and Sc (ppm) contents with mg# of clinopyroxene

The clinopyroxene in the clinopyroxene–amphibole aggregate (MAL-3) has a mg# = 0.79 and is compositionally very similar to the megacrysts MBR-2 and MBR-3 (Table 1), so that clinopyroxene from this aggregate can be considered as type 1. Clinopyroxene in the clinopyroxene–olivine aggregate (MBR-8) also belongs to type 1. In this sample, both phases are somewhat more heterogeneous than observed in the other samples.

Minor and trace element contents

Minor and trace element characteristics vary according to clinopyroxene type, and can be used to further characterise the high-Mg type 1 samples. Incompatible trace elements like REE, HSFE, Fe^{3+} and Sr increase with decreasing mg#, consistent with the clinopyroxenes having crystallised from progressively fractionated magmas, whereas compatible elements such as Sc and V decrease with decreasing mg# (e.g., Fig. 5a, b; Table 1, eTable 2).

Normalised REE patterns from all samples have a generally similar form, controlled to a large extent by the partitioning behaviour between clinopyroxene and melt. The abundances increase by about a factor of two between types 1 and 2 and between types 2 and 3 (Fig. 6a, b). Inspection of the REE patterns in type 1 clinopyroxenes reveals differences that allow further subdivision of these samples (Fig. 6a). Samples MBR-8, MBR-9 and MAL-1 have the lowest LREE and HREE concentrations and are referred as type 1a. Megacrysts MAL-2, MAL-4, MAL-5 and MBR10 (type 1b) have similarly low LREE, but have higher HREE abundances by nearly a factor of two. Most type 1b samples contain sulphide inclusions. A third type (type 1c), exemplified by samples MBR-2, MBR-3, and MAL-3, has similar HREE concentrations to type 1b, but LREE contents are distinctly elevated. In addition, type 1c clinopyroxenes possess the highest concentrations of Li, U and Th measured in this study (eTable 2, Fig. 7). This type of clinopyroxene also coexists with amphibole (i.e., MAL-3).

The REE abundances reported by Liotard et al. (1988) for clinopyroxene megacrysts from Mont Briançon and Marais de Limagne lie between the type 2 and type 3 clinopyroxenes identified in this study. This outcome can be explained by the fact that they separated clinopyroxene fragments from bulk lava samples

rather than analysing individual megacrysts. As a result, the analyses in Liotard et al. (1988) likely represent a mixture of clinopyroxene types 1, 2 and 3 present in unknown proportions.

Composition of coexisting phases in aggregates

The amphibole co-existing with clinopyroxene in sample MAL-3 is calcic and Fe^{3+}-rich ($Fe^{3+}/\Sigma Fe = 0.53$). It is a magnesiohastingsite following the classification scheme of Leake et al. (1997) and is similar in composition to the amphibole reported by Liotard et al. (1983) from the same locality (see Table 1). The Ti and alkali contents, with Na_2O higher than K_2O, are typical for amphiboles from localities in the Massif Central (Liotard et al. 1983). Trace element abundances are elevated in the amphibole compared to the co-existing clinopyroxene, except for Sc, Hf, and Zr, which occur in somewhat higher concentrations in the pyroxene (eTable 2). Although LREE are relatively higher in amphibole, the HREE abundances are essentially the same as those in the clinopyroxene (Fig. 8).

Olivine in the aggregate MRR-8 has a forsterite content of 82 ± 1 mol% and a Ni concentration of 0.13 wt%. Considering the typical composition of mantle olivine ($X_{fo} \geq 0.89$ and Ni ~ 0.3 wt% e.g., Woodland et al. 2006), the olivine in this aggregate cannot have been inherited from a peridotitic source (e.g., a disaggregated peridotite xenolith), but rather must have crystallised with the clinopyroxene.

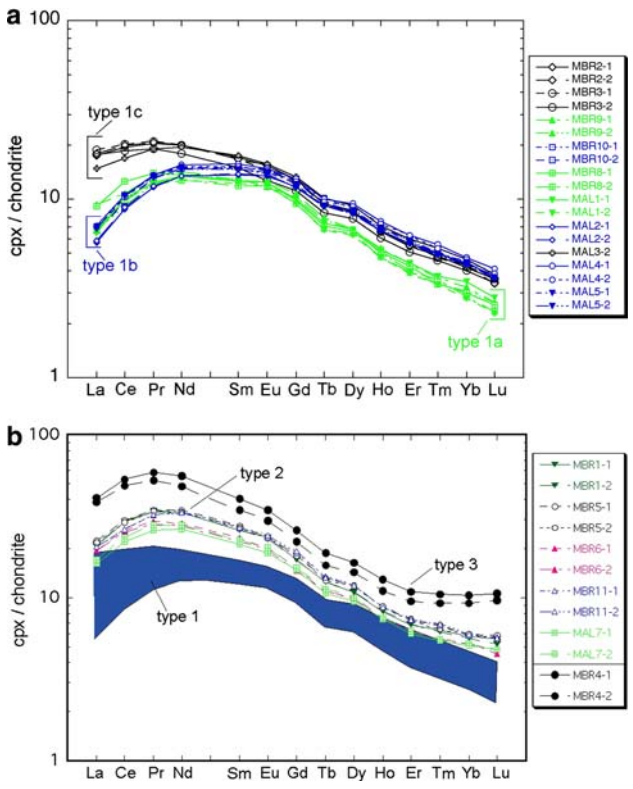

Fig. 6 REE patterns normalised to C1 chondrite (Tayor and McLennan 1985) for **a** type 1, **b** type 2 and type 3 clinopyroxenes. Note the stepwise increase in REE abundances going from type 1 to type 2 to type 3

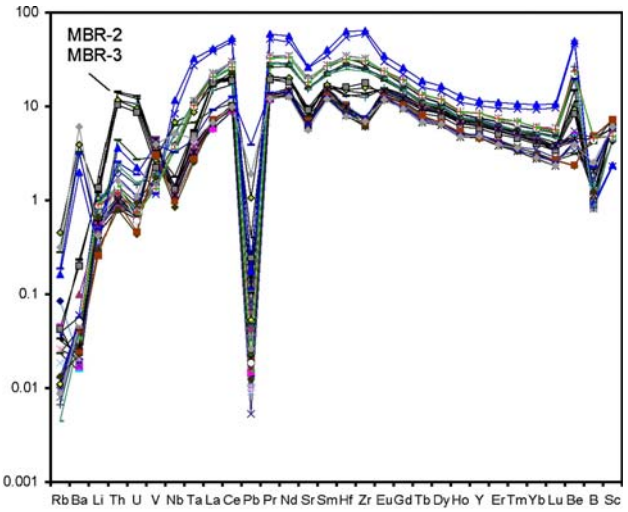

Fig. 7 Extended normalised (to C1 chondrites; Tayor and McLennan 1985) trace element diagram. Note the elevated U and Th concentrations in certain samples (see text)

Discussion

Origin of clinopyroxene

The fact that the clinopyroxenes in our suite exhibit a large range in mg# means that they could not all have crystallised from the same melt. An important question is whether any of the clinopyroxenes could have crystallised from their host magma. We can assess this by comparing the MgO/FeO of the host lavas with values calculated by combining the FeO/MgO of the megacrysts (Fe^{3+} corrected) with pertinent clinopyroxene/melt partitioning data. Lava compositions reported in Liotard et al. (1988) were recalculated assuming $Fe^{3+}/Fe^{2+} = 0.20$, as recommended by Irving and Frey (1984), yielding MgO/FeO = 1.29 and 1.30 for Mount Briançon and Marais de Limagne, respectively. For compositions similar to these lavas, Putirka et al. (1996) report Fe–Mg partition coefficients $[(FeO/MgO)_{cpx} \times (MgO/FeO)_{melt}]$ of 0.28–0.33. Assuming this range to be representative, we computed possible MgO/FeO values for the melt in which the megacrysts would be in equilibrium (Table 2). Of all the samples, only MAL-1 can arguably be considered to be in

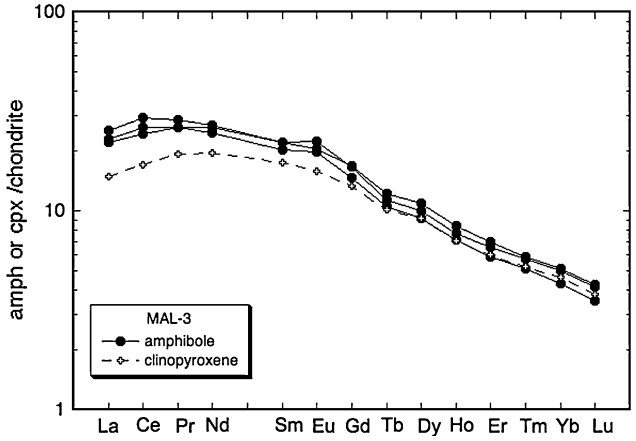

Fig. 8 Chondrite-normalised REE contents in amphibole from sample MAL-3. The pattern for the co-existing clinopyroxene is shown for reference

equilibrium with its host lava. This is an interesting result in so far as the sample has a lozenge shape, indicating reaction with the magma during transport. Of course it does not preclude the possibility that the megacryst was in equilibrium with the host magma at depth. However, this would imply that the host magma did not fractionate any further after this clinopyroxene crystallised. The clinopyroxene in sample MBR-8 yields a calculated MgO/FeO approaching that of the Mont Briançon lava, but even in this case some minor fractionation relative to the host lava composition seems to be required (Table 2). All other samples must have crystallised from melts more Fe-rich than the host lavas. This last conclusion is rather insensitive to our assumption regarding the Fe^{3+}/Fe^{2+} of the host lava. Choosing a ratio of 0.1 would reduce the MgO/FeO of the host lavas to ~1.16, which is still too Mg-rich to have been in equilibrium with the majority of the megacrysts. A higher Fe^{3+}/Fe^{2+} of 0.3 would yield a host lava MgO/FeO of ~1.48, and in this case we would conclude that even megacrysts MAL-1 and MBR-8 could not have been in equilibrium.

Normalised REE contents of the magmas from which the clinopyroxenes crystallised were calculated in a similar fashion by combining our data with the clinopyroxene-melt partition coefficients given by Zack et al. (1997). Their coefficients should be valid for the compositional range represented by our samples since they are essentially those that were experimentally determined by Hart and Dunn (1993) for alkali basalt to basanite melt compositions. The resulting melt compositions derived from clinopyroxenes MAL-1 and MBR-8 (type 1a), as well as that for MAL-2 (type 1b) are basically consistent with the limited data on the host magmas at Marais de Limagne and Mont

Table 2 Calculated MgO/FeO of parental magmas and depth of crystallisation of the clinopyroxenes

	Type	MgO/FeO[a] parent melt	Pressure[b] (kbar)
Mont Briançon			
MBR-1	2	0.49–0.58	3.0
MBR-2	1c	0.84–0.99	4.4
MBR-3	1c	0.60–0.70	5.7
MBR-4	3	0.29–0.34	2.7
MBR-5	2	0.49–0.58	3.4
MBR-6	2	0.48–0.56	4.1
MBR-8	1a	0.96–1.13	10.7
MBR-9	1a		5.8[c]
MBR-10	1b	0.80–0.94	12.4
MBR-11	2	0.58–0.69	4.0
Host lava[d]		1.29	
Marais de Limagne			
MAL-1	1a	1.09–1.28	10.6
MAL-2	1b	0.84–0.99	12.7
MAL-3	1c	0.83–0.98	6.3
MAL-4	1b	0.89–1.05	12.3
MAL-5	1b	0.89–1.05	11.9
MAL-7	2	0.45–0.53	4.0
Host lava[d]		1.30	

[a] Range calculated using partition coefficients of 0.28 and 0.33 (Putirka et al. 1996), see text

[b] Calculated after Nimis and Ulmer (1998)

[c] Calculated asumming $Fe^{3+}/\Sigma Fe = 0.3$

[d] Recalculated from Liotard et al. (1988), see text

Briançon reported by Liotard et al. (1988), suggesting that types 1a and 1b could have crystallised either directly from their host magmas or from a magma closely related in composition (Fig. 9). Considering their MgO/FeO and REE systematics, clinopyroxene types 1c, 2 and 3 must be xenocrystic with respect to the host lavas (Table 2, Fig. 9). However, genetic relationships remain a possibility.

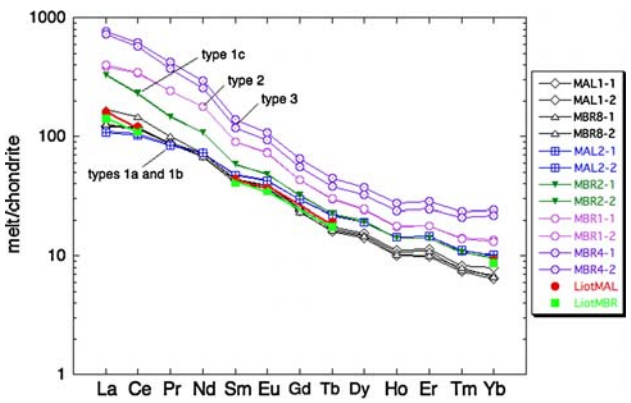

Fig. 9 Calculated chondrite-normalised (Taylor and McLennan 1985) REE patterns of parental magmas for samples representative of clinopyroxene types 1a, 1b, 1c, 2 and 3. Partition coefficients were taken from Zack et al. (1997). Also shown are normalised values for the host lavas (Liotard et al. 1988)

Systematic variations in minor and trace element concentrations with mg#, including those illustrated in Fig. 5a and b are highly suggestive of clinopyroxene types 1, 2 and 3 having crystallised from magmas that are genetically related to each other through progressive differentiation; compatible elements are systematically depleted and incompatible elements are systematically enriched with increasing differentiation (i.e., decreasing mg#). Not only the total iron content, but also the Fe^{3+} content of the melt increased significantly during differentiation (Fig. 5a). The clinopyroxene types also have very similar normalised REE patterns, with the patterns merely shifted to higher concentrations going from type 1 to type 2 to type 3 (Fig. 6b). The covariation of high field strength elements and REE with mg#, as exemplified by Hf/Sm, is further evidence that the different clinopyroxene types crystallised from genetically related magmas that had undergone progressive degrees of differentiation (Fig. 10). Type 1c clinopyroxene is an exception to this scheme, having elevated LREE such that La concentrations overlap with the type 2 samples (Fig. 6b) and Hf/Sm that departs from the general linear trend defined by the remaining samples. This, along with their relatively high Li, Th and U contents, indicates that type 1c clinopyroxenes crystallised from a somewhat more enriched batch of mafic magma than types 1a and 1b.

Pressure of crystallisation

An estimate of the pressure of crystallisation for each sample can be made by applying the geobarometer of Nimis and Ulmer (1998). Their model is valid for basic, low SiO_2 bulk rock compositions such as ours. It is important to have an accurate determination of Fe^{3+} and Fe^{2+}, as this can introduce significant errors in the calculated pressure. For example, the calculated pressure for sample MBR-3 differs by 1.2 kbar, depending on whether or not Fe^{3+} is explicitly accounted for in the calculation. Clinopyroxene types 2 and 3 record low pressures of 2.7–4.0 kbar, consistent with crystallisation under crustal conditions. In contrast, samples with high mg# (type 1) yield a range in calculated pressures from 4.4 kbar up to nearly 13 kbar (Table 2). With the exception of MBR-9, which has a vuggy appearance, the type 1a and 1b clinopyroxenes crystallised at pressures >10 kbar, indicative of mantle conditions for both the megacrysts and the basanitic magmas. The geochemically distinct type 1c clinopyroxenes all record lower pressures of 4.4–6.3 kbar, placing their crystallisation in crustal magma chambers or conduits (Table 2).

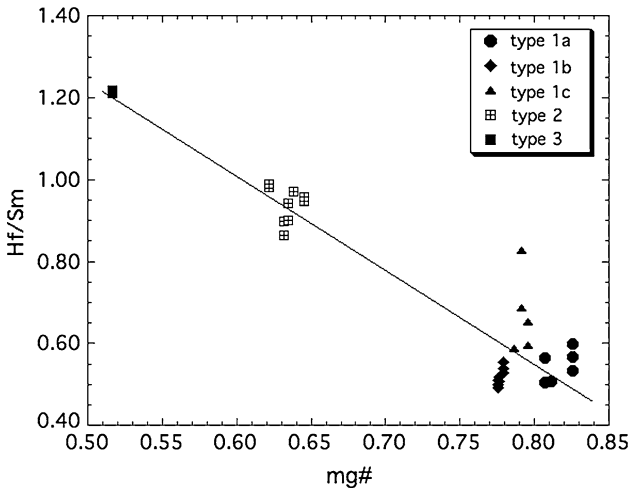

Fig. 10 Variation in Hf/Sm with mg# for the different types of clinopyroxene

Clinopyroxene–amphibole aggregate

The coexistence of clinopyroxene and amphibole in sample MAL-3 allows us the opportunity to investigate element partitioning between these two phases. Both Ti and Fe^{3+} preferentially partition into amphibole with $D^{amph/cpx}$ = 3.75 and 2.65, respectively, when calculated on a mutual basis of 24 oxygens pfu. This behaviour is not unexpected considering the crystal chemistries of the two phases. The partitioning of REE between amphibole and clinopyroxene is systematic, ranging from ~1.6 for LREE down to ~1.0 for HREE (Fig. 11). The D_{REE}-values compare very favourably with literature data from amphibole-bearing spinel peridotites (Witt-Eickschen and Harte 1994; Chazot et al. 1996) and garnet pyroxenites (Zack et al. 1997). This is particularly the case for average values derived from ten West Eifel xenoliths reported by Witt-Eickschen and Harte (1994) (note the linear scale in Fig. 11) and suggests chemical equilibration between amphibole and clinopyroxene in sample MAL-3.

The magmatic system in crust and mantle

The fact that both localities contain clinopyroxene types 1a, 1b and 1c, as well as type 2, strongly suggests that the Mont Briançon and Marais de Limagne eruptive centres are surface expressions of the same magmatic system and that the two centres could have formed more or less contemporaneously. In this context, it is important to note that the clinopyroxene types crystallised in both the crust and mantle, indicating not only a common source region for the mag-

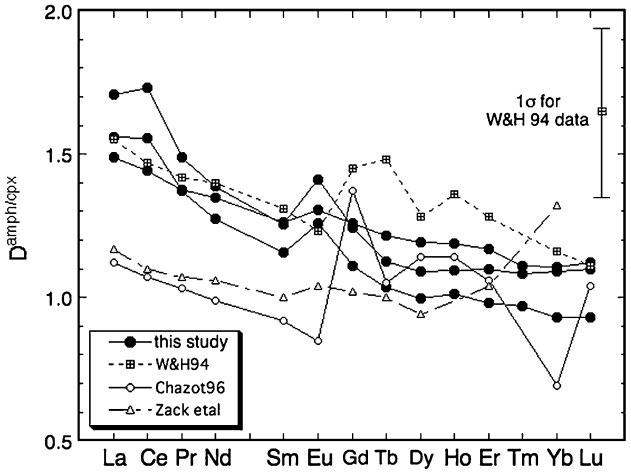

Fig. 11 REE partition coefficients for amphibole–clinopyroxene in sample MAL-3. Three separate patterns are shown, based upon different amphibole analyses, to illustrate the within-sample variation. Literature data from Witt-Eickschen and Harte (1994) (average of ten xenoliths from West Eifel), Chazot et al. (1996) (average of three xenoliths from Yemen), and Zack et al. (1997) (pyroxenites from Kakanui, New Zealand) are plotted for reference. Agreement with the literature data is very good, particularly for the Witt-Eickschen and Harte (1994) dataset (note the linear scale of the *y*-axis). The representative standard deviation in D_{REE} for the average values from Witt-Eickschen and Harte (1994) (i.e., ±0.3) is also plotted

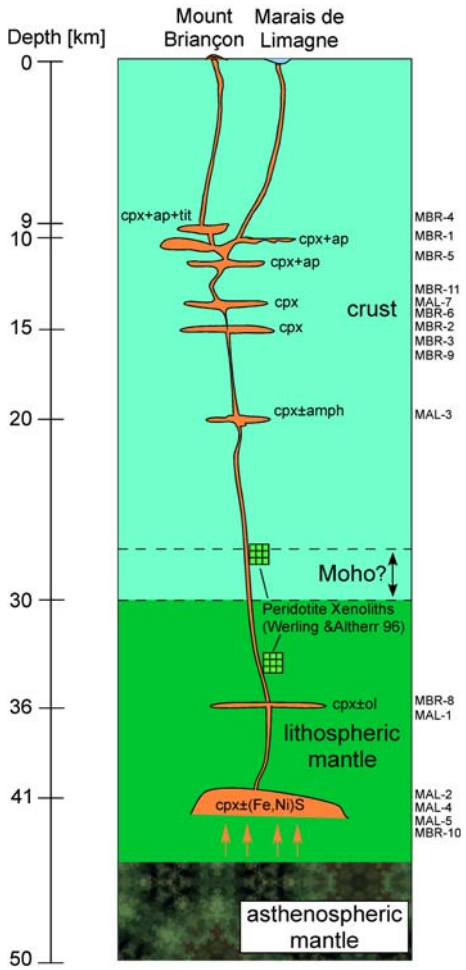

Fig. 12 Schematic section of the magmatic system underneath Mont Briançon and Marais de Limagne. The approximate depth of the clinopyroxene samples is also indicated

mas, but also that both localities share a common magmatic system at crustal levels. The similarity in host lava compositions at Mont Briançon and Marais de Limagne supports this interpretation (Table 2, Fig. 9 and see Liotard et al. 1988). Thus the suite of megacrysts and mineral aggregates provides a detailed view into the magmatic system beneath the northern part of the Devès volcanic field.

A schematic section of the magmatic system below Mont Briançon and Marais de Limagne into the mantle is presented in Fig. 12. The depth to the Moho is constrained from seismic data to lie at ~30 km (Zeyen et al. 1997). However, thermobarometric data (Ca in olivine) for a mantle xenolith from Marais de Limagne suggests a slightly shallower depth for the crust–mantle boundary (27 km for sample 34/1 from Werling and Altherr 1996). Teleseismic tomography indicates a thinned lithosphere in this part of the Massif Central, placing the lithosphere–asthenosphere boundary at ~50 km beneath the Devès volcanic field (Sobolev et al. 1996). The high-pressure type 1a and 1b clinopyroxene megacrysts yielding depths of ~40–43 km clearly formed in the mantle and most reasonably represent crystallisation from different batches of asthenospheric mafic melt that ponded in the mantle lithosphere, near the lithosphere–asthenosphere boundary. The magma from which the type 1b clinopyroxenes crystallised was locally S-saturated, leading to the formation of immiscible sulphide liquid that adhered to the surface of the growing megacrysts. Megacryst MAL-1 and the clinopyroxene–olivine aggregate (MBR-8) crystallised at somewhat shallower, but still mantle depths, possibly along a conduit wall.

The presence of mid-crustal magma chambers at various depths is indicated by the type 2 and 3 megacrysts. These chambers must have become established in advance of eruption in order to allow enough time for significant magmatic differentiation to occur. This scenario is consistent with the ''mush column'' model of Marsh (1996). The compositional systematics of megacryst types 2 and 3, along with their coexisting with apatite and apatite + titanite, respectively, suggests these two groups belong to a differentiation series

that developed within the mush column at ~10 km depth.

The type 1c clinopyroxenes (and amphibole) represent the products of crystallisation from a batch of essentially undifferentiated mantle-derived mafic melt that reached middle crustal levels. Although the higher LREE contents of these clinopyroxenes could be due in part to crystallisation at lower pressures compared to the other type 1 clinopyroxenes (i.e., P-dependent partition coefficients, Adam and Green 1994), the elevated Li, U and Th contents in the type 1c samples suggest that crustal contamination modified the trace element signature of this magma.

Considering the rather primitive lava compositions at the Mont Briançon and Marais de Limagne (Liotard et al. 1988) and the wide variety of megacryst types present at these two localities, the following interpretation for the evolution of the magmatic system and the cause of eruptions can be made. Asthenosphere-derived mafic melts that had ponded in the lithospheric mantle ascended to mid-crustal levels, where a system of magma chambers and conduits established a mush column. Here, magmas underwent various degrees of crystal fractionation, progressively evolving to become Fe-rich, more oxidised (Fe^{3+}-rich) and generally enriched in incompatible trace elements. This evolution led to crystallisation of clinopyroxene or clinopyroxene and amphibole, followed by clinopyroxene with apatite and then clinopyroxene together with apatite and titanite. The aggregate of clinopyroxene and amphibole probably represents a fragment of a crystalline crust that developed within the solidification front along a chamber or conduit wall.

Eruption was caused by a pulse of Mg-rich magma from the asthenosphere that entered the existing magmatic system, entraining clinopyroxene as megacrysts at several stages of ascent, before erupting at the surface. Magma transport from the mantle magma chambers to those in the crust must have been rapid, leading to entrainment of peridotite xenoliths in the mantle lithosphere (e.g., Werling and Altherr 1996). The occurrence of peridotite xenoliths indicates the magma must have had a short residence time, if any, at crustal levels prior to eruption. Significant residence times in crustal magma chambers have the consequences of either allowing the xenoliths to settle out and not be erupted, or giving enough time for the xenoliths to react physically and chemically with the magma, causing disaggregation and dissolution of the xenoliths (e.g., Shaw 2004). Many of the peridotite xenoliths at Mont Briançon are quite angular in form, indicating minimal reaction with the magma prior to eruption. The presence of megacrysts with compositions clearly out of equilibrium with the host lava also suggests rapid ascent and eruption before they could be completely resorbed.

The eruptive style at Mont Briançon is quite different from that at Marais de Limagne, the first being a cinder cone and the latter being a maar. This difference is most likely due to local variations in near-surface hydrology. The exact relative timing of the two eruptions is unclear and may not be resolvable by standard radiometric techniques. However, the similarities in the megacryst populations at Mont Briançon and Marais de Limagne indicate that not only are the two centres linked to the same magmatic system at depth, but also that they probably erupted nearly contemporaneously. Considering that most megacrysts in this suite are not in equilibrium with their host lava and that the variety of megacrysts is essentially the same at both localities, a significant time lag between the two eruptions can be ruled out, otherwise, most of the megacrysts would have had time to be resorbed prior to the second eruption.

Acknowledgments Jacques and Marie-Claude Kornprobst and Sarah and Gareth Woodland are thanked for their help in the field. Nicole Nuber aided in obtaining clean mineral separates for Mössbauer spectroscopy. Heidi Höfer helped with the microprobe analyses. Yann Lahaye is thanked for helping with the trace element analyses. Some of the ideas presented here benefited from discussions with Cliff Shaw and Dimitri Ionov. Michael Marks and an anonymous reviewer provided useful insights.

References

Adam J, Green TH (1994) The effects of pressure and temperature on the partitioning of Ti, Sr and REE between amphibole, clinopyroxene and basanitic melts. Chem Geol 117:219–233

Akinin VV, Sobolev AV, Ntaflos T, Richter W (2005) Clinopyroxene megacrysts from Enmelen melanophelinitic volcanoes (Chukchi Peninsula, Russia): application to composition and evolution of mantle melts. Contrib Mineral Petrol 150:85–101

Best MG (1970) Kaersutite–peridotite inclusions and kindered megacrystsin basanitic lava, Grand Canyon, Arizona. Contrib Mineral Petrol 27:25–44

Binns RA, Duggan MB, Wilkinson JFG (1970) High-pressure megacrysts in alkaline lavas from northeastern New South Wales. Am J Sci 269:132–168

Biovin P (1982) Interactions entre magmas basaltiques et manteau supérieur. Thèse d'état, Université de Clermont-Ferrand II

Bodinier JL, Guiraud M, Fabriès J, Dostal J, Dupuy C, (1987) Petrogenesis of layered pyroxenites from the Lherz, Freychinède and Prades ultramafic bodies (Ariège, French Pyrenees). Geochim Cosmochim Acta 51:279–290

Brousse R, Lefevre C (1990) Le Volcanisme en France. Masson, Paris, p 263

Canil D, O'Neill HStC (1996) Distribution of ferric iron in some upper-mantle assemblages. J Petrol 37:609–635

Chazot G, Menzies M, Harte B (1996) Determination of partition coefficients between apatite, clinopyroxene, amphibole and melt in natural spinel lherzolites from Yemen: implications for wet melting of the lithospheric mantle. Geochim Cosmochim Acta 60:423–437

Debaisieux M (1999) Volcans célèbres et méconnus du Massif Central. Editions Debaisieux, Beaumont, p 128

Dromgroole EL, Pasteris JD (1987) Interpretation of sulfide assemblages in a suite of xenoliths from Kilbourne Hole, New Mexico. In: Morris EM, Pasteris JD (eds) Mantle metasomatism and alkaline magmatism. Geol Soc Am Spec Pap 215:25–46

Goer De Herve A de, Camus G, Biovin P, Gourgaud A, Kieffer G (1991) Volcanologie de la Chaîne des Puys (Massif Central français)—Carte au 25000, 3rd edn. Parc Naturel Régional des Volcans d'Auvergne (explanatory notes), p 127

Gutmann JT (1977) Textures and genesis of phenocrysts and megacrysts in basaltic lavas from the Pinacate field. Am J Sci 277:833–861

Hart SR Dunn T (1993) Experimental cpx/melt partitioning of 24 trace elements. Contrib Minéral Petrol 113:1–8

Irving AJ (1974) Megacrysts from the newer basalts and other basaltic rocks of southeastern Australia. Geol Soc Am Bull 85:1503–1514

Irving AJ, Frey FA (1984) Trace element abundances in megacrysts and their host basalts: constraints on partition coefficients and megacryst genesis. Geochim Cosmochim Acta 48:1201–1221

Leake BE, Woolley AR, Arps CES, Birch WD, Gilbert MC, Grice JD, Hawthorne FC, Kato A, Kisch HJ, Krivovichev VG, Linthout K, Laird J, Mandarino JA, Maresch WV, Nickel EH, Rock NMS, Schumacher JC, Smith DC, Stephenson NCN, Ungaretti L, Whittaker EJW, Youzhi G (1997) Nomenclature of amphiboles: report of the subcommittee on amphiboles of the International Mineralogical Association, Commission on New Minerals and Mineral Names. Am Mineral 82:1019–1037

Liotard JM, Boivin P, Cantagrel J-M, Dupuy C (1983) Mégacristaux d'amphibole et basalts alcalins associés. Problèmes de leurs relations pétrogenétiques et géochimiques. Bull Minéral 106:451–464

Liotard JM, Briot D, Boivin P (1988) Petrological and geochemical relationships between pyroxene megacrysts and associated alkali-basalts from Massif Central (France). Contrib Mineral Petrol 98:81–90

Lorand J-P, Alard O, Luguet A, Keays RR (2003) Sulfur and selenium systematics of the subcontinental lithospheric mantle: inferences from the Massif Central xenolith suite (France). Geochim Cosmochim Acta 67:4135–4151

Luth RW, Canil D (1993) Ferric iron in mantle-derived pyroxenes and a new oxybarometer for the mantle. Contrib Mineral Petrol 113:236–248

Marsh BD (1996) Solidification fronts and magmatic evolution. Mineral Mag 60:5–40

McCammon CA, Chinn IL, Gurney JJ, McCallum ME (1998) Ferric iron content of mineral inclusions in diamond deom George Creek, Colorado determined using Mössbauer spectroscopy. Contrib Mineral Petrol 133:30–37

Merle O, Michon L (2001) The formation of the West European rift: a new model as exemplified by the Massif Central area. Bull Soc Géol Fr 172:213–221

Michon L, Merle O (2001) The evolution of the Massif Central rift: spatio-temporal distribution of the volcanism. Bull Soc Géol Fr 172:201–211

Nimis P, Ulmer P (1998) Clinopyroxene geobarometry of magmatic rocks. Part 1: an expanded structural barometer for anhydrous and hydrous basic and ultrabasic rocks. Contrib Mineral Petrol 133:122–135

Pearce NJG, Perkins WT, Westgate JA, Gorton MP, Jackson SE, Neal CR, Chenery SP (1997) A compilation of new and published major and trace element data for NIST SRM 610 and NIST SRM 612 glass reference materials. Geostand Newsl 21:115–144

Peterlongo JM, Goer de Herve A de (1978) Massif Central. Masson, Paris, p 224

Peterson R, Francis D (1977) The origin of sulfide inclusions in pyroxene megacrysts. Am Miner 62:1049–1051

Putirka K, Johnson M, Kinzler R, Longhi J, Walker D (1996) Thermobarometry of mafic igneous rocks based on clinopyroxene–liquid equilibria, 0–30 kbar. Contrib Mineral Petrol 123:92–108

Schulze DJ (1987) Megacrysts from alkalic volcanic rocks. In: Nixon P (ed) Mantle xenoliths. Wiley, Chichester pp 433–451

Shaw CSJ (2004) The temporal evolution of three magmatic systems in the West Eifel volcanic field, Germany. J Volc Geotherm Res 131:213–240

Shaw CSJ, Eyzaguirre J (2000) Origin of megacrysts in the alkaline lavas of the West Eifel volcanic field, Germany. Lithos 50:75–95

Sobolev SV, Zeyen H, Stoll G, Werling F, Altherr F, Fuchs K (1996) Upper mantle temperatures from teleseismic tomography of Franch Massif Central including effects of composition, mineral reactions, anharmonicity, anelasticity and partial melt. Earth Planet Sci Lett 139:147–163

Sobolev VN, McCammon CA, Taylor LA, Snyder GA, Sobolev NV (1999) Precise Mössbauer milliprobe determination of ferric iron in rock-forming minerals and limitations of electron microprobe analysis. Am Mineral 84:78–85

Taylor SR, McLennan SM (1985) The continental crust, its composition and evolution: an examination of the geochemical record preserved in sedimentary rocks. Blackwell, Oxford, p 312

Van Achterbergh E, Ryan CG, Jackson SE, Griffin WL (2001) Data reduction software for LA-ICP-MS. In: Sylvester P (ed) Laser-Ablation-ICPMS in the earth sciences—principles and applications. Miner Assoc Can (short course series) 29:239–243

Wass SY (1979) Multiple origins of clinopyroxenes in alkali basaltic rocks. Lithos 12:115–132

Werling F, Altherr R (1996) Thermal evolution of the lithosphere beneath the French Massif Central as deduced from goethermobarometry on mantle xenoliths. Tectonophysics 275:119–141

Wilkinson JFG (1975) Ultramafic inclusions and high-pressure megacrysts from a nephelinite sill, Nandewar Mountains, northeastern New South Wales, and their bearing on the origin of certain ultramafic inclusions in alkaline volcanic rocks. Contrib Mineral Petrol 51:235–262

Wilshire HG, Schwarzmann EC, Trask NJ (1980) Amphibole rich veins in lherzolite xenoliths, Dish Hill and Deadman Lake, California. Am J Sci 280A:576–593

Wilson M, Downes H (1991) Tertiar–Quaternary extension-related alkaline volcanism in western and central Europe. J Petrol 32:811–849

Witt-Eickschen G, Harte B (1994) Distribution of trace elements between amphibole and clinopyroxene from mantle peridotites of the Eifel (Western Germany): an ion-microprobe study. Chem Geol 117:235–250

Witt-Eickschen G, Seck H, Reys C (1993) Mulitple enrichment processes and their relationships in the subcrustal lithosphere beneath the Eifel (Germany). J Petrol 34:1–22

Woodland AB, Kornprobst J, McPherson E, Bodinier J-L, Menzies MA (1996) Metasomatic interactions in the lithospheric mantle: petrologic evidence from the Lherz Massif, French Pyrenees. Chem Geol 134:83–112

Woodland AB, Kornprobst J, Tabit A (2006) Ferric iron in Orogenic Lherzolite Massifs and controls of oxygen fugacity in the upper mantle. Lithos 89:222–241

Zack T, Foley SF, Jenner GA (1997) A consistent partition coefficient set for clinopyroxene, amphibole and garnet from laser ablation microprobe analysis of garnet pyroxenites from Kakanui, New Zealand. N Jb Mineral Abh 172:23–41

Zeyen H, Novak O, Landes M, Prodehl C, Driad L, Hirn A (1997) Refraction-seismic investigations of the northern Massif Central (France). Tectonophys 275:99–117